

A Primer on Reaction–Diffusion Models in Embryonic Development

Matthew J Thompson, *School of Biomedical Engineering, Purdue University, West Lafayette, Indiana, USA*

Hans G Othmer, *School of Mathematics, University of Minnesota, Minneapolis, Minnesota, USA*

David M Umulis, *School of Agricultural and Biological Engineering, Purdue University, West Lafayette, Indiana, USA*

A fundamental problem in developmental biology is understanding how complex patterns and organised tissues develop from a small group of nearly identical cells. A wealth of experimental data has exposed the complexity of the molecular networks guiding cellular decisions of organisation and patterning – networks whose output evolves over space and time as development progresses. Integrating this data into reaction–diffusion (RD) mathematical models that describe the spatiotemporal dynamics of molecular species during development provides a rigorous approach to test the plausibility of hypothesised mechanisms guiding pattern formation, to understand how the complexity is regulated and to optimise experimental design. RD modelling provides a complementary mode of inquiry that both depends on and informs experimental research. RD systems are used in developmental biology to model morphogen-mediated pattern formation.

Introduction

The role of mathematical models in development

During the early stages of metazoan development, a zygote undergoes rapid mitotic proliferation during the blastula stage, which

eLS subject area: Developmental Biology

How to cite:

Thompson, Matthew J; Othmer, Hans G; and Umulis, David M (August 2018) A Primer on Reaction–Diffusion Models in Embryonic Development. In: eLS. John Wiley & Sons, Ltd: Chichester.

DOI: 10.1002/9780470015902.a0026599

Advanced article

Article Contents

- Introduction
- Processes Modelled by Reaction–Diffusion Equations
- Examples of Reaction–Diffusion Models
- Considerations for Model Implementation
- Summary
- Acknowledgements
- Funding
- Related Articles

Online posting date: 24th August 2018

is followed by cellular movement, differentiation and germ layer specification during the gastrula and later stages. Throughout this early process, zygotic gene expression is regulated by a precisely coordinated flurry of maternal and zygotic cues (mRNA (messenger ribonucleic acid) distributions, cytokines, etc.), thereby regulating pattern formation, cellular proliferation, differentiation and morphogenesis. These same processes are employed again during organogenesis. The patterns serving as the output for these analyses are the spatially restricted gene expression domains that arise as an effect of signalling from mobile instructing molecules called morphogens. This is all accomplished in a spatially and transiently reproducible manner that is robust to environmental variation. These properties of robustness and reproducibility are puzzling and difficult, if not impossible, to resolve from a classical, exclusively experiment-based approach.

Fundamental questions of pattern formation during development must then be addressed through the specification and quantitative characterisation of the spatiotemporal programs controlling the formation and interpretation of the morphogen distributions. This stage of analysis is where mathematical modelling can make significant contributions. The judicious application of mathematical models integrated with imaging and biophysical data enables new mechanisms of pattern formation to be tested and vetted, yielding novel insights into the core processes governing development.

In this pedagogical article, an introductory description of the prerequisite concepts and techniques used in these approaches will be provided. The basic equations governing reaction–diffusion (RD) systems are developed in **Box 1**, and an example of how alternative transport mechanisms may be approximated as diffusion is shown in **Box 2**. It is common to assume that a reaction–transport phenomenon can be approximated as RD (Kicheva *et al.*, 2007), but such simplification carries a caveat. The use of effective diffusion as an approximation for transport mechanisms is often based on a highly simplified model of reality and thus may not provide mechanistic insight into the actual mode of transport (Bollenbach *et al.*, 2005; Gonzalez-Gaitan and Jülicher, 2014; Lin and Othmer, 2017). Similarly, unknown reaction kinetics may be approximated

with phenomenological forms that reduce aspects of a model's mechanistic descriptive power. An apt aphorism for this word of caution is that 'all models are wrong, but some are useful' (Box, 1979). It is the responsibility of the modeller to appropriately frame the scope and context of the questions being addressed with the model at hand. With these concepts in mind, examples of how RD models are used to describe and test hypotheses of mechanisms for morphogen-mediated pattern formation in diverse developmental contexts are provided. These examples illustrate the utility of an iterative approach between experimentation and mathematical modelling which neither approach can provide on its own.

Reverse engineering of development

To understand the role of RD equations in addressing questions in developmental biology, it is helpful to use a mental framework typified by engineering analogies. An organism can be thought to be the product of an evolutionarily engineered system where dynamical networks of components interact to accomplish some performance objective. Such objectives include pattern formation, positional specification and precision, scale invariance, growth control and robustness to signal perturbation and parameter variation (Umulis and Othmer, 2015). Identifying components of such a network and describing their relationships are akin to reverse engineering, which attempts to deconstruct systems or objects and determine the design of the system and how the system works. In this framework, the concepts of *forward* and *inverse* problems and *top-down* and *bottom-up* approaches to reverse engineering are important to understand.

In a forward problem, one knows the components of the system and inputs and predicts an output. A living organism undergoing development executes a forward problem. Input components – including the genome, maternal mRNA, DNA (deoxyribonucleic acid) and RNA (ribonucleic acid) polymerases – are subject to the biophysics and biochemical kinetics governing their activity to produce the embryo's phenotype and morphology (Jaeger *et al.*, 2004; Lobo *et al.*, 2014). Conversely, an inverse problem uses a measured output and the postulated architecture of the system to determine the inputs used to generate that output. These inputs are not necessarily unique, and it may be the case where several, many or infinite sets of inputs can produce a single output state. This is a property evident in diverse biological systems using different mechanisms across species to accomplish similar objectives (Mdluli, 2017; Zinski *et al.*, 2017).

The process of reverse engineering a biological system can be undertaken using a full range of bottom-up and top-down approaches. Both approaches begin by identifying performance objectives met by the system. A bottom-up approach then proceeds with an effort to identify the most relevant molecular components within a certain context through methods such as '-ome' analysis (genome, transcriptome, proteome, epigenome, lipidome, etc.). Once a subset of molecules is flagged among the global population through differential expression, the molecules may be studied at higher resolution to build hypotheses of how they achieve certain emergent properties. A top-down approach seeks to identify parsimonious (i.e. minimal) models to produce

these observed properties. These are useful for proposing theoretical mechanisms which may serve as a falsifiable basis for targeted empirical investigation and later refinement or elimination. From either direction, a way to model the network dynamics is needed to investigate mechanistic questions.

RD equations are useful in both top-down and bottom-up approaches to describe aspects of patterning in development at different levels of detail. RD equations are a type of partial differential equation (PDE) used to describe transient and spatially dependent morphogen distributions and their dynamic interactions with other molecules. RD equations are immediately applicable from a top-down approach to match observations qualitatively when little is known about the underlying structure. On the other hand, they can also be used to provide a quantitative framework for testing hypothesised inputs and mechanisms on their ability to produce a specific set of outputs. In between top-down and bottom-up approaches, RD equations may also be used in 'middle-out' approaches to see if the currently known components are sufficient or to suggest new factors if key behaviours are missing. For example, they could be used to propose additional regulatory molecules or interactions not yet identified in a process sufficient to drive the network dynamics towards a performance objective (Umulis *et al.*, 2006).

Processes Modelled by Reaction–Diffusion Equations

RD equations are built from three classes of terms. The first is the *transport* of components through mechanisms that may be described as diffusion. The others are *production* and *clearance* of components through interactions within the system or through independent reactions. These equations have the following form for each component:

$$\begin{aligned} &\text{Rate of change of the local concentration} \\ &= \text{transport} + \sum \text{production} - \sum \text{clearance} \end{aligned}$$

Production terms are the reactions and interactions that increase a component's concentration, and clearance terms are those that decrease its concentration. Specifying these terms is done by hypothesising the biophysical and biochemical mechanisms involved in morphogen dynamics. The transport term is usually represented by diffusion, but the utility of these equations may be extended beyond the small subset of biological processes truly controlled by free diffusion. Effective diffusion may approximate systems where free diffusion is inhibited or active transport mechanisms influence the concentration profile (Bollenbach *et al.*, 2005; Umulis and Othmer, 2013).

The end goal, however, is not simply to describe the distribution dynamics of morphogens, but to use this information to answer specific scientific questions. For instance, the set of RD equations may be used to demonstrate the sufficiency of a proposed set of mechanisms to produce certain biological phenomena or to test the efficacy and side effects of a proposed therapeutic treatment in a disease model. Other routes of investigation involve

Table 1 Examples of morphogen-mediated patterning models using RD equations in diverse systems

Context	Model description	Primary questions addressed	Reference
Bicoid in <i>Drosophila</i>	Single component, linear, SDD	Can physiologically relevant diffusion coefficients facilitate the good fit between the SDD model and biophysical Bicoid data?	Gregor <i>et al.</i> (2007)
Bmp in zebrafish	Multicomponent, nonlinear	Is the BMP shuttling mechanism for gradient formation conserved between <i>Drosophila</i> and zebrafish?	Zinski <i>et al.</i> (2017)
Nodal/Lefty in zebrafish	Two-component activator–inhibitor, nonlinear	Does differential clearance or differential diffusivity facilitate the Nodal signalling gradient?	Müller <i>et al.</i> (2012)
Shh in mouse neural tube patterning	Multicomponent, nonlinear	What role do non-steady-state dynamics of network components play in morphogen-mediated tissue patterning?	Saha (2006)
Gap genes in <i>Drosophila</i>	Multicomponent, nonlinear	Discrimination among model regulatory topologies through a novel fitting method	Perkins <i>et al.</i> (2006)
Wnt/Dkk in mouse hair follicle formation	Two-component activator–inhibitor, nonlinear	Is a Turing-type RD model sufficient to explain hair follicle pattern formation? (Note: here, reaction–diffusion is used synonymously with the specific Turing mechanism.)	Sick <i>et al.</i> (2006)
Fgf in zebrafish	Single component, linear	Is the simple source–sink mechanism sufficient to describe the Fgf8 morphogen profile?	Yu <i>et al.</i> (2009)
Bmp and Wnt in mouse digit formation	Three component, linear and nonlinear analysis	Is a Turing-type RD model sufficient to explain digit formation in the forelimb, and what are the implicated molecules?	Raspopovic <i>et al.</i> (2014)
Bmp in <i>Drosophila</i>	Multicomponent, nonlinear	How do BMP-receptor binding enhancement and positive feedback affect robustness and bistability?	Umulis <i>et al.</i> (2006)

questions regarding the information-carrying capacity encoded in a morphogen distribution and how the information carried in this signal is interpreted by cells locally and globally. Morphogens commonly modelled with RD equations include TGF- β , BMP, NODAL, WNT, SHH and FGF (**Table 1**). Examples will be explored in a following section.

Derivation of RD equations for morphogen patterning

Using the qualitative version of the mass-balance equation from the previous section, a mass balance is developed in **Box 1** that includes the reaction and transport terms leading to the basic equation (B.1.3).

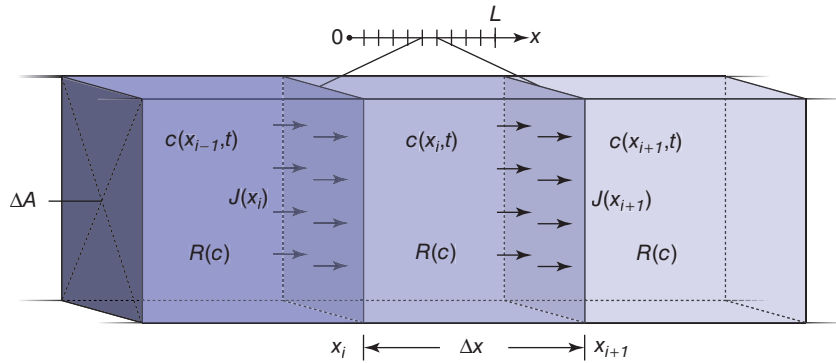
In models of biological systems, more complexity must be considered than shown in the derivation of **Box 1**, that is there may be:

1. *Multiple mobile species.* Several mobile morphogens may be involved in a patterning model, represented by the vector $\mathbf{c} = (c_1, \dots, c_i, \dots, c_n)$.
2. *Multidimensional transport.* Morphogen transport in higher dimensions involves fluxes in the y and z directions (across boundaries of ΔA_y and ΔA_z), expressed using the dot product

between the gradient operator $\nabla = (\partial/\partial x\hat{\mathbf{i}}, \partial/\partial y\hat{\mathbf{j}}, \partial/\partial z\hat{\mathbf{k}})$ and the flux vector $\mathbf{J} = (J_x, J_y, J_z)$ for each $c_i \in \mathbf{c}$.

3. *Stationary species.* Some molecular species may be immobilised, and their concentrations are represented by the vector $\mathbf{s} = (s_1, \dots, s_j, \dots, s_m)$. When modelling 3D diffusible morphogens, an important distinction between 3D- and 2D-bound immobile molecules must be made when implementing these equations (e.g. ubiquitous immobile extracellular matrix (ECM) molecules in 3D and diffusible transmembrane receptors in 2D). In some instances, bound complexes will continue to diffuse on the cell membrane, requiring the gradient operator and a definition of flux on the cell membrane. Here, we will assume a spatially uniform distribution of these components within the domain based on an assumption that the total concentration of immobile species is constant (Umulis *et al.*, 2008).
4. *Reactions.* The net effect of reactions governing each component may be represented by the summation of individual reactions $R_{c,i}(\mathbf{c}, \mathbf{s}, \mathbf{p})$ and $R_{s,j}(\mathbf{c}, \mathbf{s}, \mathbf{p})$. Each of these R terms represents a single reaction that is a function of the other components in the system (\mathbf{c} and \mathbf{s}) and parameters (\mathbf{p}). These may also include zeroth-order reactions which are not dependent on any concentrations.

Box 1 Derivation of transport continuity equation with reaction in one dimension



In the simplest case of a one-dimensional system on the domain $\Omega = [0, L]$ that involves a single morphogen, we can develop the spatiotemporal morphogen concentration along a region of interest, $c(x, t)$, as follows. Imagine the system to be divided into n small control volumes of length Δx and cross-sectional area ΔA , where the concentration within each volume is uniform. Within the i th volume, given by $\Delta A \cdot \Delta x$, the change in quantity of the morphogen over a small time period Δt is equal to the difference between the quantity at the initial time, t_τ , and final time, $t_\tau + \Delta t$ (or equivalently, $t_{\tau+1}$). This is equal to the sum of the flux J into and out of the volume through boundary areas at positions x_i and $x_i + \Delta x$ plus the rate of reaction within the volume $R(c)$. The reaction term represents the net rate of morphogen creation or destruction as it depends on local concentration within that volume. Flux and chemical reactions take place over the course of a small time, Δt . Thus, the quantity of morphogen within this i th volume is:

$$\Delta A \cdot \Delta x \cdot (c(x_i, t_\tau + \Delta t) - c(x_i, t_\tau)) = \Delta A \cdot \Delta t \cdot (J(x_i) - J(x_i + \Delta x)) + \Delta A \cdot \Delta x \cdot \Delta t \cdot R(c) \quad (\text{B.1.1})$$

Checking units:

$$\left([L^2] \cdot [L] \cdot \left[\frac{M}{L^3} \right] \right) = \left([L^2] \cdot [t] \cdot \left[\frac{M}{L^2 t} \right] \right) + \left([L^2] \cdot [L] \cdot [t] \cdot \left[\frac{M}{L^3 t} \right] \right) = [M]$$

Terms in square brackets denote generalised units of M (quantity), L (length) and t (time). It is a useful practice to check units often when mathematically formalising physical systems.

Dividing each term in equation (B.1.1) by $\Delta A \cdot \Delta x \cdot \Delta t$ yields:

$$\frac{c(x_i, t_\tau + \Delta t) - c(x_i, t_\tau)}{\Delta t} = \frac{J(x_i) - J(x_i + \Delta x)}{\Delta x} + R(c) \quad (\text{B.1.2})$$

Taking the limit as $\Delta t \rightarrow 0$ and as the number of control volumes along the system $n \rightarrow \infty$, $\Delta x \rightarrow 0$, these may be expressed as the partial derivative with respect to t and x . This allows the concentration, flux and reaction rate to be expressed as continuous quantities, yielding the most basic RD PDE:

$$\frac{\partial c}{\partial t} = -\frac{\partial J}{\partial x} + R(c) \quad (\text{B.1.3})$$

The solution, $c(x, t)$, may be determined when boundary conditions at $x=0$ and L and initial conditions at $t=0$ are known or specified.

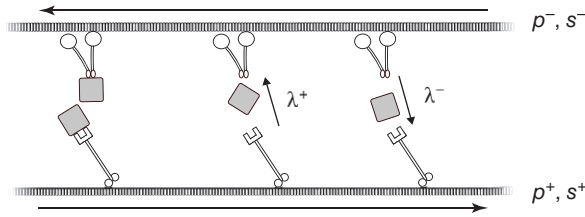
The contributions lead to the following extended form of equation (B.1.3) for each morphogen $c_i \in c$ and immobile species $s_j \in s$:

$$\frac{\partial c_i(x, y, z, t)}{\partial t} = -\nabla \cdot \mathbf{J}_i + \sum_{c_j \in c} R_{c_i, j}(c, s, p) \quad (1)$$

$$\frac{\partial s_j(t)}{\partial t} = \sum_{s_j \in s} R_{s_j}(c, s, p) \quad (2)$$

Here, $\nabla \cdot \mathbf{J}_i$ represents all forms of transport, both active and passive, where ∇ is the differential operator or gradient defined as $\mathbf{i}\partial/\partial x + \mathbf{j}\partial/\partial y + \mathbf{k}\partial/\partial z$. However, these equations are not useful for modelling biological systems in their current form. The transport term must reflect experimental data to be physiologically relevant and therefore must be re-expressed. The flux of a single morphogen c_i in one dimension resulting from the passive process of free diffusion may be described by Fick's first law of diffusion: $J_{i,x} = -D_i(\partial c_i/\partial x)$, where D_i is the diffusion coefficient,

Box 2 Approximation of active transport equation along microtubules as effective diffusion



Microtubule-mediated molecular transport provides an effective means of intracellular transport for moving components within the cell, and in some cases between nuclei in a syncytium (e.g. in the *Drosophila* blastoderm embryo). Assuming isotropic microtubule orientation (i.e. no cellular polarisation), this active transport process may be approximated as effective diffusion, derived here in one dimension as in Othmer *et al.* (1988).

As in the figure above, suppose that protein cargo travels along a microtubule to the right (positive motion) at constant speed, but at any time it can change direction and travel to the left (negative motion) – and *vice versa* – by jumping between dynein and kinesin motor proteins. A model tracking the probability density of proteins travelling in a positive or negative direction may be expressed as:

$$\frac{\partial p^+}{\partial t} + \frac{\partial(s^+p^+)}{\partial x} = -\lambda^+p^+ + \lambda^-p^- \quad (\text{B.2.1})$$

$$\frac{\partial p^-}{\partial t} - \frac{\partial(s^-p^-)}{\partial x} = \lambda^+p^+ - \lambda^-p^- \quad (\text{B.2.2})$$

Here, $p^+(p^-)$ are proteins travelling in the positive (negative) direction with speed $s^+(s^-)$ switching from positive to negative directed motion at a rate λ^+ (*vice versa* for λ^-). In general, s^\pm and λ^\pm can vary in space. In the special case, where $s^+ = s^- = s$ and $\lambda^+ = \lambda^- = \lambda$, equations (B.2.1) and (B.2.2) can be combined to give the telegraph equation for total particle density $p = p^+ + p^-$:

$$\frac{\partial^2 p}{\partial t^2} + 2\lambda \frac{\partial p}{\partial t} = s^2 \frac{\partial^2 p}{\partial x^2} \quad (\text{B.2.3})$$

Taking the limit as $\lambda \rightarrow \infty$ and $s \rightarrow$ with $s^2/2\lambda \equiv D_{\text{eff}}$ as the constant effective diffusion coefficient, the diffusion equation for molecular transport by velocity jump may be used as an approximation for microtubule-mediated transport:

$$\frac{\partial p}{\partial t} = \underbrace{\left(\frac{s^2}{2\lambda} \right)}_{D_{\text{eff}}} \frac{\partial^2 p}{\partial x^2} \quad (\text{B.2.4})$$

Equation (B.2.4) is appropriate only when s and λ are spatially constant. This illustrates how simple diffusion equations may be used to approximate active transport processes. In cases where speeds and turning rates are nonuniform, cargo concentration becomes nonuniform due to directed or biased effective diffusion. For more detail on nonuniform processes, see Erban and Othmer (2005).

or diffusivity, of species c_i . The negative sign indicates that the flux is from high to low concentration. Extending to 3D, this becomes $\mathbf{J}_i = -D_i \nabla c_i$. Substituting into equation (1) and assuming constant diffusion coefficients yields:

$$\frac{\partial c_i}{\partial t} = \underbrace{D_i \nabla^2 c_i}_{\text{Transport}} + \underbrace{\sum_{c_j \text{ Rxns}} R_{c_i}(c, s, p)}_{\text{Production \& Clearance}} \quad (3)$$

$$\frac{\partial s_j}{\partial t} = \underbrace{\sum_{s_j \text{ Rxns}} R_{s_j}(c, s, p)}_{\text{Production \& Clearance}} \quad (4)$$

This form may apply phenomenologically to modes of transport beyond free diffusion when viewed on a long time scale, as illustrated in **Box 2** (Othmer *et al.*, 1988). The correct conditions, in this case, require dilute solutions of constant viscosity and isotropic random directed motion for this form to be valid

(Crowder, 1997). More generally, the diffusion coefficient may not be constant, and thus the flux takes the form $\nabla \cdot D_i \nabla c_i$.

A mobile component's diffusivity affects the spatial range of its influence. This parameter may be determined experimentally by fluorescence recovery after photobleaching (FRAP) (Carisey *et al.*, 2011) and fluorescence correlation spectroscopy (FCS) or fluorescence cross-correlation spectroscopy (FCCS) (Ries and Schwille, 2012). These techniques provide data relevant to very different contexts of time and length scales. FCS measures very small volumes and is appropriate for the determination of a molecule's free diffusion, whereas FRAP is done over a larger volume spanning several or many cells and is useful for determining effective diffusion (Wang *et al.*, 2016). This raises several difficulties in extracting diffusion coefficients and kinetic parameters.

Along with the experimental determination of a morphogen's diffusivity, it is essential to understand quantitatively the biochemical mechanisms and reactions controlling the concentration profile, both intracellularly and extracellularly. Furthermore, when specifying the regulatory terms, the system's biochemical mechanisms must be known or hypothesised. These formulations further add to the system's degrees of freedom through uncertain parameters or uncertainty in the mechanisms themselves. These reactions can be described by mass-action kinetics, Michaelis–Menten or reversible Michaelis–Menten kinetics, Hill's equation, allosteric and cooperativity and other methods as detailed in textbooks elsewhere.

Examples of Reaction–Diffusion Models

Systems of RD equations display diverse dynamics, depending on the mechanisms described by the reaction terms. The models studied most thoroughly have been classified based on the interactions in these mechanisms.

A brief description of the Turing model and positional information

RD equations are used to describe pattern formation in systems ranging from cell biology to ecology and are fundamental to the two characteristic concepts for developmental pattern formation established by Alan Turing and Lewis Wolpert – Turing pattern formation (Turing, 1952) and positional information (PI) (Wolpert, 1969). Initially, Turing and PI models of pattern formation were proposed from a top-down perspective – establishing thought paradigms through which pattern formation during development is often interpreted. Currently they are also used as a framework for bottom-up approaches. Though these theories are distinct in origin, they are closely related. A thorough conceptual description of these mechanisms and how patterns may arise by each individually or in combination can be found elsewhere (Green and Sharpe, 2015). Broadly speaking, there is more control over the spatial pattern in PI, but the range of patterns is more restricted than in Turing mechanisms.

Briefly, the Turing model describes a system where a spatial pattern emerges from an initially uniform state. In a homogenous 'well-mixed' system, the kinetic mechanism is asymptotically stable – that is, in the long run, it will reach a time-invariant equilibrium state. In the Turing mechanism, the interaction of reaction and diffusion destabilises the uniform state, leading to a spatially nonuniform steady state (Turing, 1952). Specific examples of RD mechanisms driving pattern propagation include an activator–inhibitor pair (**Figure 1a**) and substrate depletion. Examples of the former with minor revisions are provided in this article.

The theory of PI proposes a mechanism of pattern formation that requires a prepattern or initial asymmetry that determines the localisation of a morphogen source or sink. Morphogens then diffuse from the source and create a concentration gradient along some body axis (Wolpert, 1969). Cells along the gradient sense their local morphogen concentrations to infer their position relative to the global scale, and cellular decisions in the form of downstream gene activation are made based on the concentration requirements defining the boundaries between regions (**Figure 1b**).

Turing activator–inhibitor models

The classical two-component Turing mechanism consists of an activator and inhibitor (**Figure 1a**). In the original conception of this model, the activator activates both itself and the inhibitor, and the inhibitor blocks the activator. The inhibitor has a significantly larger diffusion coefficient than the activator such that it extends its negative influence on the activator beyond the activator's reach of local autoenhancement. This mechanism enables the establishment of a repeating pattern in the spatial concentrations of both components. Examples of this type of pattern traditionally discussed include the stripes and spots in fur, scales and skin – although recently, Turing-like mechanisms have been implicated in important morphogenetic processes during early development as well. For instance, it was confirmed that in zebrafish, the Nodal/Lefty system that determines mesendoderm specification during the blastula stage (Müller *et al.*, 2012) as well as left–right asymmetry (Schier, 2009) functions because of disparities in the diffusion coefficients for these components. The inhibitor (Lefty) has roughly 3- to 20-fold greater diffusion coefficients than the activator (Nodal), depending on the specific molecules compared (Nodal: Cyclops and Squint; Lefty: Lefty1 and Lefty2) (Müller *et al.*, 2012).

The equations used to model this system are nonlinear because of the interactions between the components, as shown below:

$$\frac{\partial A}{\partial t} = D_A \nabla^2 A + \phi_A + \rho_A \frac{A^2}{I + \epsilon} - k_A A \quad (5)$$

$$\frac{\partial I}{\partial t} = D_I \nabla^2 I + \rho_I A^2 - k_I I \quad (6)$$

Here, A is the activator (Nodal), I is the inhibitor (Lefty), ρ_A and ρ_I are cross-reaction coefficients, k_A and k_I are decay rate constants and ϕ_A is a constant production term for A . The form presented here is one of the several RD equations for activator–inhibitor

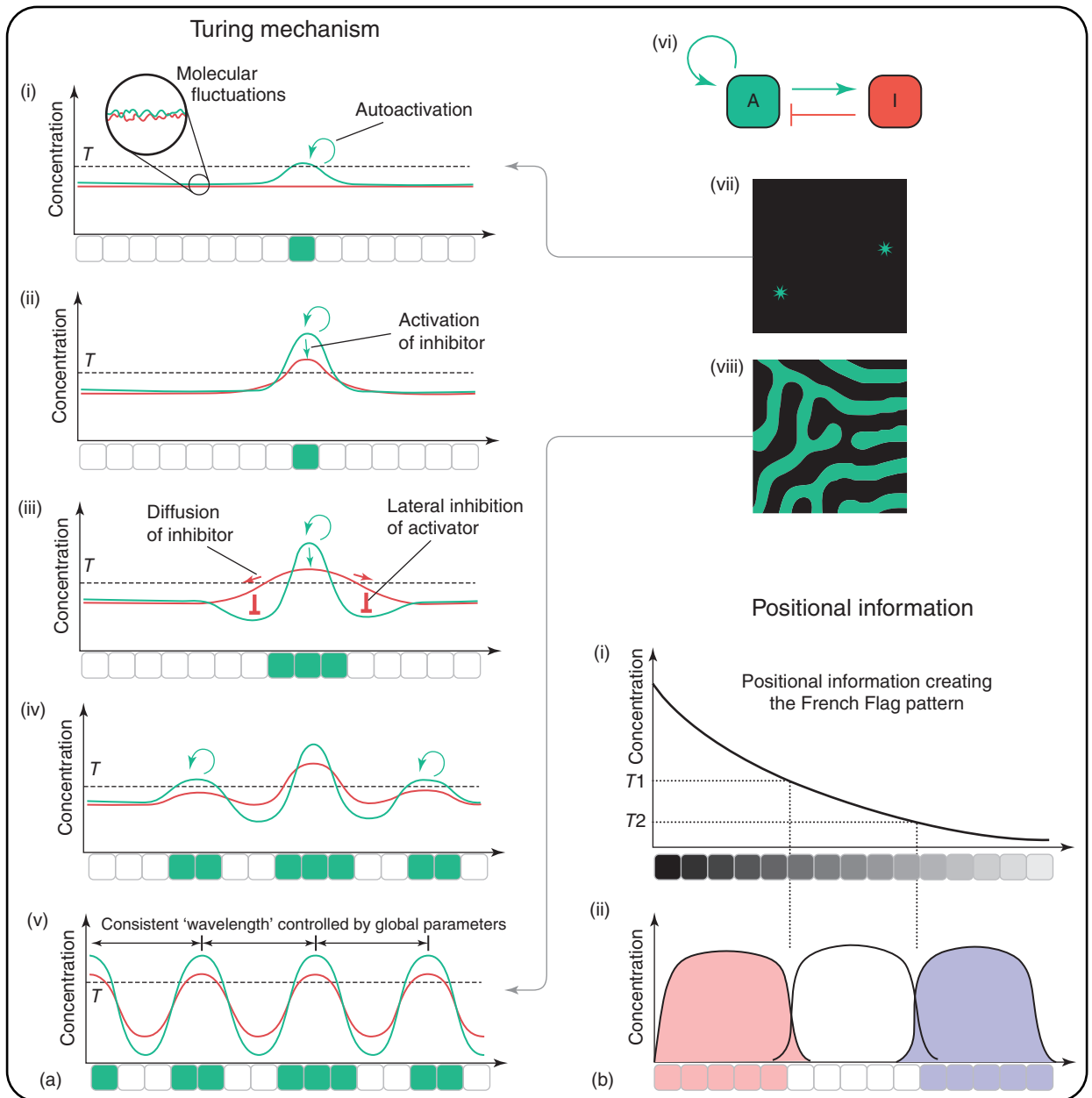


Figure 1 The *Turing* model and the positional information model of morphogen-mediated pattern formation. The *x* axes indicate the spatial position along a line of cells. (a) In the *Turing* model, stochastic fluctuations induce random deviations from a uniform steady state in the concentration of a diffusive signalling molecule (green) which are amplified and propagated due to the reactions between the components (vi) to form a periodic pattern that may collide with other similar patterns with different orientations and starting positions (vii), generating intricate designs (viii). Once a concentration threshold is reached, cells respond by initiating downstream gene transcription and taking on a ‘green’ phenotype. (b) In Wolpert’s model of positional information, (i) a signalling molecule concentration gradient emanates from a source, (ii) where multiple phenotypes (red, white or blue) may result based on concentration thresholds. Source: Green, <http://dev.biologists.org/content/142/7/1203>. Licensed under CC BY 4.0.

Turing mechanisms and is referred to as the Gierer–Meinhardt system (Gierer and Meinhardt, 1972). This is a ‘top-down’ phenomenological model, and in its original form had $\epsilon = 0$, which is unrealistic for low levels of *I*. Here, we add the parameter ϵ to obviate this issue. The experimental result presented by this

article identifying the differential diffusivities between Nodal and Lefty is important for its confirmation that the theoretical requirement for this characteristic in an activator–inhibitor pair is indeed satisfied in this biological example. However, this is referred to as a ‘*Turing*-like’ mechanism in this article because it is not truly a

Turing mechanism, as was suggested in Green and Sharpe (2015). The authors of the Nodal/Lefty study are careful to point out that ‘Nodal and Lefty expression is biased by prepatterns, and the tissue response is restricted by size and time scales’ (Müller *et al.*, 2012). In other words, there is no initial symmetry to break due to the prepattern of maternal Nodal-activating transcription factors along the blastula margin, and there is no observable periodicity in gene expression because of the size and timescale limitations. However, this activator–inhibitor pair could reasonably be expected to autoregulate from symmetrical initial conditions if there was no prepattern present and form a periodic pattern under different spatiotemporal conditions. The Nodal/Lefty system in this context therefore may satisfy conditions of sufficiency for classification as a bona fide Turing mechanism, but the actuality of the biological system more accurately fits a PI system with Gierer–Meinhardt reactions.

Digit patterning in the limb bud is also a morphogenetic system where Turing mechanisms have been proposed (Newman and Frisch, 1979). Although detailed mathematical analysis has shown the 1979 model to be incorrect (Othmer, 1986), evidence has been found in the mouse for a three-component network with Turing instability controlling this system. In this model, Bmp, Sox9 and Wnt are the primary nodes controlling patterning, and Fgf signals and Hoxd13, as illustrated in **Figure 2**. The latter may enable the onset of initial instability and scale invariance (Raspopovic *et al.*, 2014). The evolution of the primary components is governed by the following equations:

$$\frac{\partial \text{Sox9}}{\partial t} = \phi_{\text{Sox9}} + k_2 \text{Bmp} - k_3 \text{Wnt} - (\text{Sox9})^3 \quad (7)$$

$$\frac{\partial \text{Bmp}}{\partial t} = D_{\text{Bmp}} \nabla^2 \text{Bmp} + \phi_{\text{Bmp}} - k_4 \text{Sox9} - k_5 \text{Bmp} \quad (8)$$

$$\frac{\partial \text{Wnt}}{\partial t} = D_{\text{Wnt}} \nabla^2 \text{Wnt} + \phi_{\text{Wnt}} - k_7 \text{Sox9} - k_9 \text{Wnt} \quad (9)$$

Here, the ϕ terms represent basal production or inputs. Though biologically unrealistic, the cubic Sox9³ in equation (7) was added to ‘guarantee a symmetrical saturation of Sox9 around the steady-state Sox9₀ = 0’, where this saturation ‘represents the maximum transcriptional rate of Sox9’ to prevent unbounded growth. The authors acknowledge that this is unrealistic, though

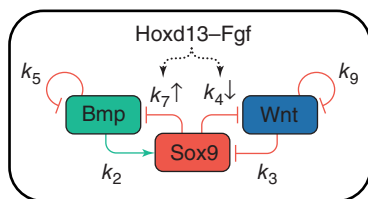


Figure 2 The three-component Bmp–Sox9–Wnt PI-driven Turing network guiding digit patterning described by the base equations (7–9). Positional information provided by Hoxd13–Fgf expression modulates the suppression of Wnt and Bmp by Sox9, initiating Turing instability, which enables the initiation and propagation of a self-regulating pattern.

its qualitative effects are necessary for the model, and its form does not alter their conclusions. The equations were solved on a growing finite element mesh, which was hard-coded to mimic the overall limb bud shape during outgrowth without regard to mechanisms controlling this growth. Initial conditions were set to homogeneous values for Sox9, Bmp and Wnt, with noise added to each component. The self-regulating dynamics resulting from these core equations created randomly oriented striped patterns of Sox9 on the growing limb bud. When the model was modified to incorporate Fgf (expressed in the apical ectodermal ridge along the limb bud margin that controls outgrowth) and Hoxd13 expression domains as well, a regular radial Sox9 pattern emerged closely resembling the out-of-phase wild-type expression between Sox9 and Wnt/Bmp, which underlies the patterning of digits. Fgf and Hoxd13 are proposed to modulate the negative interactions between Sox9 and Bmp and between Sox9 and Wnt through the constants k_4 and k_7 , respectively. These parameters were chosen to be targets of Fgf and Hoxd13 because screening simulations indicate that proportionately varying them with the Fgf and Hoxd13 concentrations caused an increase in the pattern wavelength, aligned orientation of the stripes along the gradient and afforded scale invariance. However, there is yet no explanation of a mechanism that may relate these components with their associated parameters. In this model, the onset of diffusion-driven Turing instability for the three primary components only comes about in regions of Hoxd13 expression, which only occurs in regions of Fgf expression. This incorporates a component of PI driven by Fgf upstream of the Turing network. The authors proceeded to support their model by predicting dynamics under perturbed conditions with Wnt and Bmp pathways blocked, and the simulations appeared to be qualitatively similar to experimental results. In addition, it is necessary for Bmp to diffuse more quickly than Wnt as Bmp effectively acts as an indirect inhibitor for Wnt through Sox9, though as we will soon discuss, further modelling has shown that this may not be the case.

Although two-component networks are thought to require differential diffusivity to be self-organising with the inhibitor diffusing faster than the activator, a theoretical analysis of three- and four-component Turing networks has shown that differential diffusivity is not the only mechanism by which self-organising patterns can arise when a nondiffusive species is included (Marcon *et al.*, 2016). This work explores two additional network classes: one that allows for but does not require equal diffusivities and another that is entirely independent of diffusivity. No new examples of these alternative networks have yet been demonstrated in developmental biology, and though much of this was previously known in general (Othmer, 1986), these insights were used by the authors to reanalyse the Lefty/Nodal and Wnt/Bmp/Sox9 systems discussed here. In the Lefty/Nodal system, a nondiffusive component representing pSmad2/3 activation was added, and two possible topologies were identified that could meet the constraints imposed on the system. The analysis of this new three-component network reclassifies the Lefty/Nodal system as one where differential diffusivity between activator and inhibitor is not a strictly necessary condition, though the empirically observed diffusivities act to make the system more robust. In the limb bud model, the three-component network was

changed to a five-component network to incorporate pSmad1/5/8 and β -catenin as nondiffusive nodes with Sox9. Opposing Bmp expression and Bmp activity was seen when β -catenin indirectly inhibited Sox9 through pSmad rather than the direct relationship in the three-component network between Wnt (thus presumably β -catenin) and Sox9. Their analysis also showed that the three-component network did not actually require differential diffusivity as previously thought as long as Wnt and Bmp clearance rates are not equal. It will be interesting to see future experimental and modelling work identifying other developmental systems making use of these proposed Turing mechanisms.

Models with prepattern

Though presently known biological examples of genuine Turing mechanisms are in somewhat short supply, there are many instances where diffusing morphogens demonstrate Wolpert's theory of PI in developing systems. This section will explore a progression of increasingly complex PI models including the source–sink model, synthesis–diffusion–degradation (SDD) model and larger nonlinear models.

Source–sink model

In its original form, the source–sink model is the simplest proposed morphogen-mediated RD model. This theoretical model consists of a morphogen generation term at a source point and an elimination term at a sink point with only diffusion elsewhere (Crick, 1970). In one dimension at steady state, this creates a linearly decreasing gradient from source to sink. However, no such system has been observed in biology, and biologically useful models referencing this mechanism involve one or more adjustments to the original formulation. This model may be attributed to systems where the source and sink are spread over a small region. Recently, the Bmp gradient patterning the zebrafish dorsal–ventral axis was shown to use such a distributed source–sink mechanism (Pomreinke *et al.*, 2017; Zinski *et al.*, 2017). Commonly, models will be referred to as source–sink models though they more accurately fit the description of a SDD model, as in the Fgf8 gradient in zebrafish embryos (Yu *et al.*, 2009).

Synthesis–diffusion–degradation model

The protein Bicoid (Bcd) in *Drosophila* was the first protein formally classified to function as a morphogen (Driever and Nüsslein-Volhard, 1988; Frohnhöfer and Nüsslein-Volhard, 1986). This protein is translated from maternally supplied mRNA localised around the anterior tip of the embryo and diffuses from there to provide PI along the anterior–posterior axis. Its profile can be seen in **Figure 3**, as in Grimm *et al.* (2010). This gradient was first modelled to address the question of developmental scale invariance using a slightly altered version of the source–sink model called the SDD model (Gregor *et al.*, 2005). The SDD model differs from the source–sink model in that the clearance domain is not restricted and may be ubiquitous, or its rate may be dependent on the concentration dynamics of another molecule. Assuming *bcd* mRNA to be concentrated at a point at the anterior

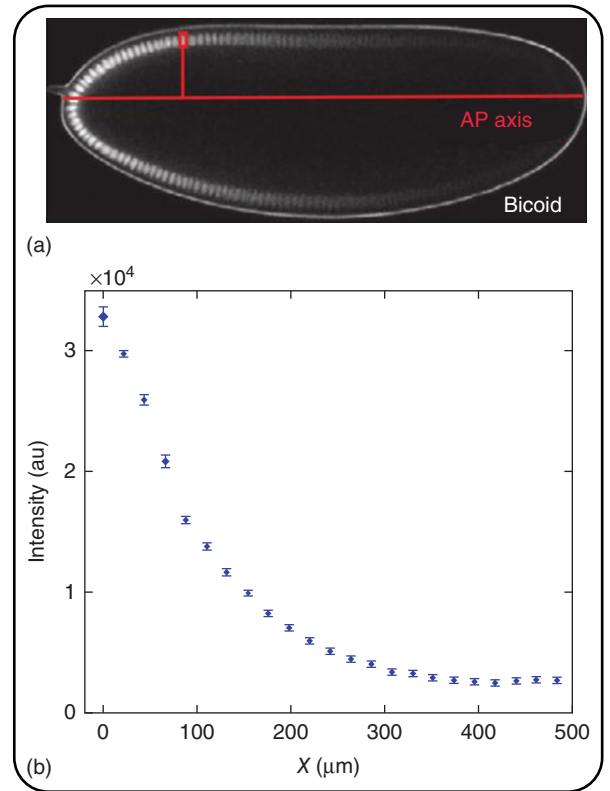


Figure 3 The *Bicoid* morphogen gradient. (a) Confocal image of nuclear localised Bicoid gradient along the *Drosophila* AP axis. (b) Semiquantitative signal intensity data along the length of the egg following the exponentially decaying profile seen in synthesis–diffusion–degradation models. Adapted with permission from Grimm *et al.* (2010). © Company of Biologists.

pole, Bcd protein was modelled along one dimension with a constant linear decay rate, k :

$$\frac{\partial c}{\partial t} = D \frac{\partial^2 c}{\partial x^2} - kc \quad (10)$$

Here, production gives rise to a constant flux boundary condition at $x=0$ ($-\partial c/\partial x(0)=J$), and there is a no-flux boundary condition at $x=L$ ($\partial c/\partial x(L)=0$). At steady state ($\partial c/\partial t=0$), equation (10) simplifies to:

$$\frac{\partial^2 c}{\partial x^2} = \frac{kc}{D} \quad (11)$$

On a spatial domain $0 \leq x \leq L$, the nondimensionalised equilibrium solution to this second-order ordinary differential equation (ODE), where $\xi = x/L$ is:

$$c(\xi) = \lambda J \left[\frac{e^{(2-\xi)/\lambda} + e^{\xi/\lambda}}{e^{2/\lambda} - 1} \right] \quad (12)$$

The term $\lambda = \sqrt{D/k}$ is the length constant. If the morphogen production rate is assumed to be constant, and c_0 is the original

concentration at $\xi=0$, then the length constant is the distance between the source and the point at which the concentration has dropped to c_0/e . Equation (12) can then be simplified under steady-state conditions and for the diffusive range of most morphogens (Umulis, 2009).

$$c(\xi) \approx c_0 e^{-\xi/\lambda} \quad (13)$$

This simple model matches the exponential decay profile seen by imaging Bcd distribution, but crucially only for unrealistically large values of D , as was pointed out in a follow-up study (Gregor *et al.*, 2007). Previous work had detected a pre-existing gradient of *bcd* mRNA at the anterior end of the embryo (St Johnston *et al.*, 1989), and though this feature was not accounted for in the SDD model, the model brought into question the still widely held assumption that Bcd protein was secreted from a point source at the anterior pole of the embryo. This was done by showing that the biophysical parameters required for this assumption to match imaging data did not match measured values. Later, the mRNA gradient was proposed to pattern the Bcd protein gradient in its entirety (Spiro *et al.*, 2009) or in concert with its protein diffusion (Little *et al.*, 2011). In the latter study, the SDD model was also extended to allow for temporally varying parameters over several nuclear cycles, resulting in simulations that fit data very tightly over several time points.

Models leading to scale invariance

Even in networks composed of few components, the incorporation of nonlinear terms may lead to complex dynamics that are not readily understood intuitively from the network topology. Nonlinear equations are also often analytically not solvable in general and require the use of numerical approaches to generate approximate solutions. The complexities raised by these points are compounded by the combinatorial explosion of possible topologies resulting even from simple theoretical systems, further establishing the need for computational analysis. For example, a molecule interacting with a morphogen may affect its transport, production, clearance or a combination thereof (as shown in the general form of RD equations) and may be nonlinearly dependent on one or more other components. The breadth of expressive power resulting from these interdependent reactions may be appreciated through a theoretical analysis of the relationships within such a simple two-component system composed of a freely diffusing morphogen and modulator (Umulis and Othmer, 2013). In this model, either component may have a positive, negative or neutral effect on the diffusivity, production rate and clearance rate of the other (Figure 4). This generates $3^6 = 729$ permutations of possible network topologies between the two components. When autoenhancement and autoinhibition of these rates are considered, it becomes $5^6 = 15\,625$.

This theoretical two-component morphogen–modulator system is an example of top-down analysis of combinatorial nonlinear networks. It was recently explored with the aim to constrain the topological landscape of networks to only those serving the performance objective of scale invariance (Othmer and Pate, 1980). In this analysis, the morphogen is defined as a freely diffusing molecule encoding PI secreted from a source at one end of

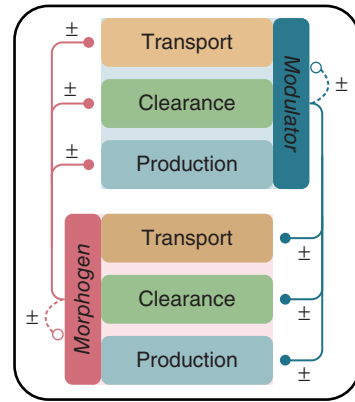


Figure 4 A theoretical morphogen-modulator two-component system. Dashed lines indicate autoregulation for either component’s own transport, clearance or production not analysed in the cited work.

a one-dimensional domain. The modulator is either bound uniformly along the domain or freely diffusing. If diffusive, it is either secreted from the same source as the morphogen, secreted from a source opposite the morphogen or uniformly secreted along the domain. The reaction topologies explored include all non-auto-regulatory relationships of positive or negative influence on the other component’s production, clearance or diffusivity, as in Figure 4. That is, these terms for the morphogen, c , are functions of a modulator, m , and vice versa.

$$\frac{\partial c(x, t)}{\partial t} = \frac{\partial}{\partial x} \left(D_c(m) \frac{\partial c}{\partial x} \right) + R_c(c, m) \quad (14)$$

$$\frac{\partial m(x, t)}{\partial t} = \frac{\partial}{\partial x} \left(D_m(c) \frac{\partial m}{\partial x} \right) + R_m(m, c) \quad (15)$$

Analysis using these RD equations of nonlinear coupled PDEs investigated how the various regulatory arrangements influence the system’s ability to maintain the relative morphogen concentration when subjected to variable length scales. An example result is that, of the 729 possible topologies for freely diffusing morphogen and modulator, fewer than 6% can maintain scale invariance for any case of modulator production (Karim, 2017).

A subset of these scale invariant topologies well represented in biological systems are those exhibiting ‘expansion-repression’ feedback (Ben-Zvi and Barkai, 2010). This subset includes all topologies where the morphogen represses an ‘expander’, and the expander enhances morphogen signalling through any direct or indirect mechanism, whether increased diffusion, increased production or decreased clearance. Nonlinear terms are introduced when diffusion, production or clearance of one component depends on the concentration of the other. Another network shown to exhibit scale invariance is the ‘long-range accumulation and feedback’ mechanism proposed to act between Chordin and Sizzled proteins during *Xenopus* development (Inomata *et al.*, 2013). This network shares similarities with the expansion–repression relationship, though detailed theoretical analysis of the mathematical relationships among various scaling mechanisms has yet to be conducted.

Facilitated diffusion

A more bottom-up approach for investigating the mechanisms of morphogen gradient formation is to closely integrate experimental data with theoretical models. A set of ‘core equations’ is established including the primary actors of the signalling network and the interactions and independent reactions that must be present. Additional terms are added individually and/or in combination to test various mechanistic hypotheses. Simulations are validated against wild-type and mutant quantitative imaging data to determine the best performing set of mechanisms and potentially suggest experiments for further validation.

An example of such an approach may be found in a study investigating *Drosophila* dorsal–ventral axis patterning by heterodimeric ligands formed by the vertebrate BMP homologues Decapentaplegic (Dpp) and Screw (Scw) (Umulis *et al.*, 2010). This study made many predictions, and the focus here will be on the analysis of how collagen binding influences signal gradient formation by facilitating diffusive complex formation. The authors made use of the experimental results (Wang *et al.*, 2008) to model the effects of collagen binding. Further experiments were later conducted to confirm the mechanism (Sawala *et al.*, 2012). This serves as an illustrative example of the iterative paradigm by which experiments and computational models complement each other and enable the generation of insights neither can produce on their own.

In this system, illustrated in **Figure 5**, signalling (i.e. ligand–receptor binding) is blocked when Dpp–Scw ligands bind with the diffusible inhibitors Short gastrulation (Sog, secreted laterally) and Twisted gastrulation (Tsg, secreted dorsally), forming a Dpp–Scw/Sog/Tsg complex. The formation and transport of this inhibited complex was postulated to act as a ‘shuttling’ mechanism, extending the range of Dpp–Scw

diffusion. An additional modulator is the metalloprotease Tolloid (Tld, secreted dorsally), which degrades Sog when it is bound to Dpp–Scw. Signalling is activated by free Dpp–Scw binding to its receptor complexes. These dynamics are described by the following system of equations:

$$\frac{\partial B}{\partial t} = D_B \nabla^2 B + \phi_B(x) - k_3 I \cdot B + k_{-3} IB + \lambda Tld \cdot IB - k_5 B \cdot R + k_{-5} BR \quad (16)$$

$$\frac{\partial S}{\partial t} = D_S \nabla^2 S + \phi_S(x) - k_2 S \cdot T + k_{-2} I \quad (17)$$

$$\frac{\partial T}{\partial t} = D_T \nabla^2 T + \phi_T(x) - k_2 S \cdot T + k_{-2} I + \lambda Tld \cdot IB - \delta_T T \quad (18)$$

$$\frac{\partial I}{\partial t} = D_I \nabla^2 I + k_2 S \cdot T - k_{-2} I - k_3 I \cdot B + k_{-3} IB \quad (19)$$

$$\frac{\partial IB}{\partial t} = D_{IB} \nabla^2 IB + k_3 I \cdot B - k_{-3} IB - \lambda Tld \cdot IB \quad (20)$$

$$\frac{dBR}{dt} = k_5 B \cdot R - k_{-5} BR - \delta_E BR \quad (21)$$

$$R_{tot} = R + BR \quad (22)$$

Here, B (for BMP) is the Dpp–Scw ligand heterodimer concentration, T is the Tsg concentration, I is the inhibitor (Sog–Tsg heterodimer) concentration, IB is the bound ligand–inhibitor concentration, BR is the bound ligand–receptor concentration, R is

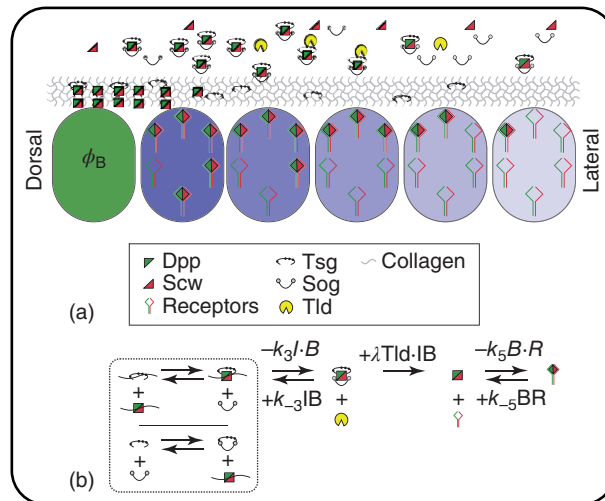


Figure 5 Bmp signalling in *Drosophila*. (a) Dpp molecules secreted from a source represented by the green nucleus are prohibited from diffusion through binding with collagen. Upon shuttling complex formation with Dpp–Scw/Sog/Tsg, it can diffuse, creating a concentration gradient along the syncytium. The inhibitory complex is broken by Tld, enabling the Dpp–Scw heterodimer to bind its receptors and initiate downstream signalling. Fading blue nuclei represent decreasing downstream Bmp target gene transcription. (b) Reactions controlling Bmp signalling in *Drosophila* with terms from equation (8). In the dashed box, the order of reactions for the Dpp shuttling complex is distinguished. Either diffusible Sog and Tsg bind before complexing with Dpp–Scw, or Tsg binds collagen, then Dpp and then Sog completes the complex formation.

the unbound receptor concentration, R_{tot} is the total receptor concentration, D_i is the diffusion coefficient for species i , \mathbf{x} is the Cartesian position vector, k_j and k_{-j} are the forward and reverse reaction rates for reaction j , δ_T is the Tsg degradation rate, δ_E is Dpp–Scw degradation rate by endocytosis and λ_{Tld} is the Tld process rate. With boundary and initial conditions, this system may be solved numerically by the finite-difference approximation. For a given biochemical reaction, experimental binding rates may be unknown and must be approximated, though data may exist for similar reactions in other model systems to aid in approximations. It is assumed that the BR profile correlates with the downstream signalling state of the system, which is inferred from phosphorylated Mad (pMad) immunostaining data.

From the core equations, additional terms or equations were added depending on hypothesised mechanisms of signal profile formation (such as the influence of collagen), and further analysis was performed on the effect of embryo geometry and mechanisms that may produce scale invariance. Model performance was evaluated based on faithful representation of quantitative pMad imaging data of mutant and wild-type embryos.

Umulis *et al.* (2010) ascertained that using *in vitro* data for BMP-inhibitor binding in zebrafish (Rentzsch, 2006) causes the models to perform quite poorly and created a model whereby collagen enhances shuttling by improving inhibitor binding, as suggested by experimental data. Indeed, models incorporating this postulated mechanism match imaging data much more closely. Furthermore, the binding order among Dpp–Scw, Sog, Tsg and collagen was investigated. In binding order 1, Sog binds Tsg before binding to collagen-bound Dpp–Scw, thereby mobilising the shuttling complex. In binding order 2, Sog binds collagen-bound Dpp–Scw before being released by binding with Tsg. Slightly better alignments with data are produced for binding order 1 simulations compared to binding order 2. Follow-up experiments were conducted by the same group generating the original Dpp and Sog collagen-binding data to show that collagen does indeed act as an intermediate component enhancing shuttle complex assembly (Sawala *et al.*, 2012), although their data suggests that the binding order showing slightly worse model performance is the actual biochemical process – that is, experimental data suggests that Dpp–Scw and Sog independently bind collagen IV, where they then bind to each other and are released when Tsg binds Sog (poorer model performance) rather than Sog binding Tsg before Sog binds to Dpp–Scw (better model performance). This indicates that the computational models, while accurate in their prediction of collagen's role in the process, require slightly more biochemical detail or perhaps slightly varied parameters to correct for the binding-order mismatch. Again, these three studies illustrate the interdependence and feedback between experiments and computational models that drive knowledge in developmental biology forward.

Surprisingly, two independent groups have recently published complementary evidence showing that this facilitated diffusion or shuttling mechanism in *Drosophila* is not conserved in zebrafish, and that the blastula-stage dorsal–ventral Bmp gradient in the zebrafish is better explained by a source–sink mechanism (Pomreinke *et al.*, 2017; Zinski *et al.*, 2017). These studies make use of light-sheet and confocal microscopy, respectively, to monitor the dynamics of fluorescently tagged Bmp2b protein dynamics

as a benchmark to test mechanistic RD models against. They show that the Bmp antagonist Chordin acts as a somewhat distributed dorsal sink to the ventrally secreted and diffusive Bmp2b, where it was previously widely thought to serve as a shuttling mechanism similar to the Sog–Tsg heterodimer in the *Drosophila* system. This exemplifies the ability of experimentally informed computational modelling to rectify inaccurate long-held assumptions.

Considerations for Model Implementation

When implementing a model, it is important to consider its distribution, interpretation, reproducibility and extensibility. The components and context of a model should be annotated to avoid ambiguity, and the syntax should be easily acquired by those wishing to replicate results. To these ends, a community standard has been established called the systems biology markup language (SBML; original publication: Hucka *et al.*, 2003) to facilitate the creation, sharing, reproduction and extension of biological models. A growing repository of models following this standard are available through The BioModels Database (original publication: Le Novere, 2006; website: <https://www.ebi.ac.uk/biomodels-main>). These items should be considered when developing a custom model using a scripting language such as MATLAB, Mathematica or Python and when using third-party software packages.

A well-maintained and evolving platform of note for integrating SBML models into systems involving spatial considerations is CompuCell3D (CC3D; original publication: Swat *et al.*, 2012; <http://www.compuCell3d.org>). Other relevant simulation frameworks include Chaste (<http://www.cs.ox.ac.uk/chaste>), CellSys, (<http://msysbio.com>), EPISM (<http://tigacenter.bioquant.uni-heidelberg.de/episim.html>), VirtualLeaf (<https://code.google.com/p/virtualleaf>), Biocellion (<http://biocellion.com>), Morpheus (<http://imc.zih.tu-dresden.de/wiki/morpheus>), OpenCMISS (<http://physiomeproject.org/software/openccmiss>) and LBIBCell (<https://bitbucket.org/tanakas/lbibcell>), all of which are discussed in greater detail elsewhere (Tanaka, 2015). In addition, the sensitivities and optimisation of biochemical kinetic and biophysical parameters may constitute a major portion of the analysis workload in such models, though this discussion is outside the scope of this article.

Summary

Performance objectives in developmental pattern formation such as robustness to perturbation, reproducibility and scale invariance are crucial aspects of developmental biology. The nuanced nature of how various morphogen networks have been shown to achieve these objectives attests to the need for precise, quantitative interpretation of experimental data, which may be managed by iteratively integrating data and RD models. A generalised workflow for a modelling project is described in **Figure 6**. **Table 1** provides a diverse set of examples where

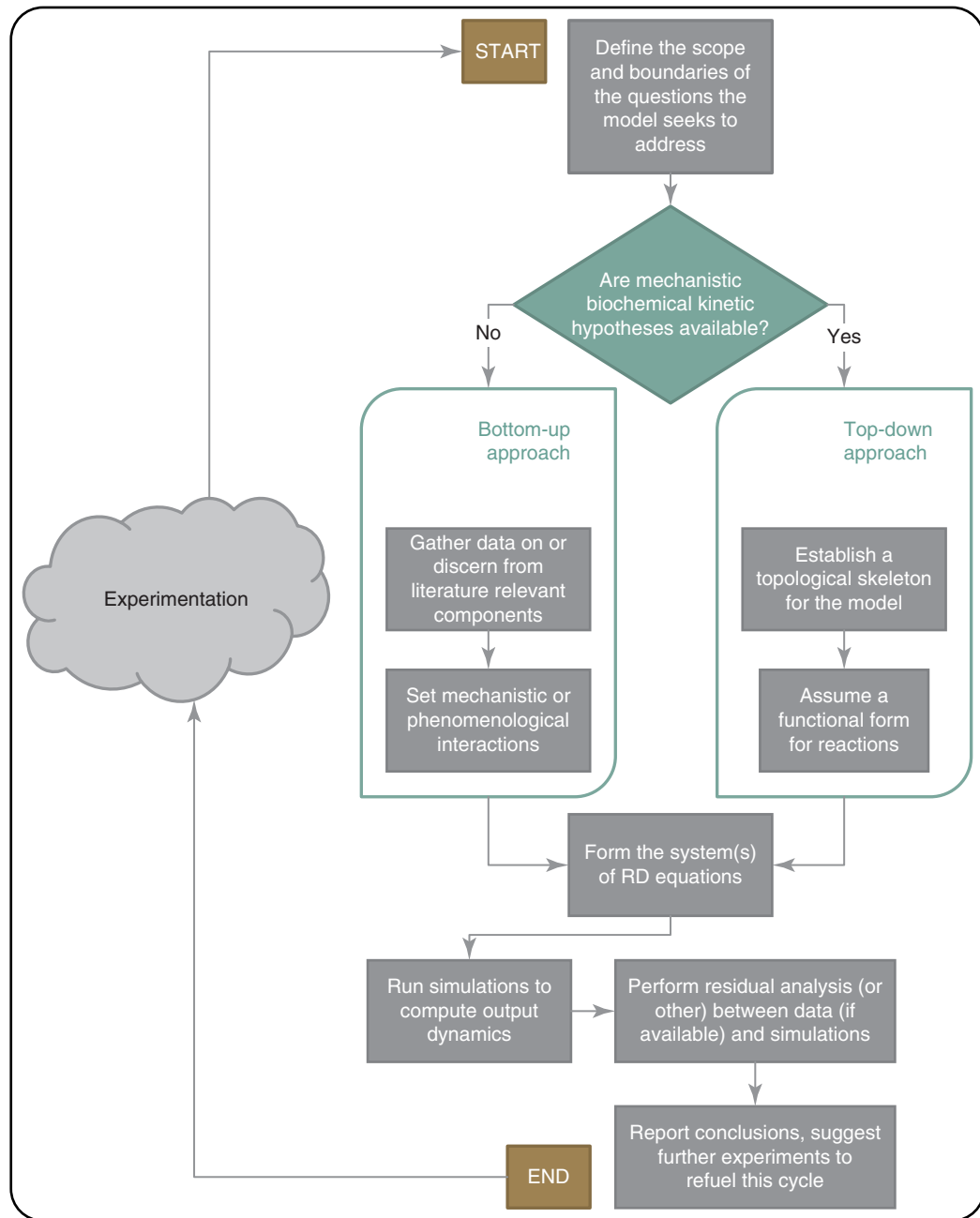


Figure 6 Generalised workflow for modelling morphogen systems using RD equations. The starting step involves asking and answering questions such as: “What objective function(s) is/are observed in the system?” “What mechanisms are known, assumed, postulated or missing?” “What data exist or need to be acquired to proceed?” “Is treating transport as pure diffusion appropriate?” The choice to pursue a top-down or bottom-up approach depends on the level of theoretical abstraction appropriate for the system. Once the system’s dynamics have been compared to data of these dynamics, the cycle may continue.

RD equations have been used to probe developmental systems, illustrating the broad reach and relevance of RD models for furthering scientific investigation in developmental biology. Spatial and temporal aspects of embryonic development are meaningful and cannot be neglected if a deeper understanding of developmental systems is to be attained. In the absence of

prioritised training in more advanced mathematics and physics in university biology curricula, it is to the advantage of students and researchers to develop these skills independently to gain a more complete understanding of the systems they are passionate about. Incorporating computational analysis using RD methods into the developmental biology lab will make possible the

conception and testing of hypotheses that would otherwise have been inaccessible, enabling new mechanisms to be discovered, and improving progress in the field (Erban and Othmer, 2005).

Acknowledgements

Much appreciation is due to Xu Wang, Ph.D. and Ye Bu, Ph.D., postdoctoral researchers in the Umulis lab, for their helpful comments, insights and aid in figure preparation.

Funding

This publication was supported by the Eunice Kennedy Shriver National Institute of Child Health and Human Development and the National Institute of General Medical Sciences of the National Institute of Health under award numbers R01GM029123 to HGO and R01HD073156 to DMU. The content is solely the responsibility of the authors and does not necessarily represent the official views of the National Institutes of Health.

Related Articles

Developmental Biology: Mathematical Modelling of Developmental Positional Information

Glossary

Bottom-up approach An approach to network and mechanism hypothesis building with a primary priority on comprehensive component identification followed by inductive, phenomenological model building and an ancillary priority on theoretical network principles. This is the bioinformatics approach.

Forward problem A process where outputs are determined by input components undergoing operations.

Inverse problem A process where inputs are determined or inferred by the outputs produced by operations.

Morphogen A biochemical substance controlling tissue gene expression patterns and morphogenesis through spatially and transiently nonuniform concentrations.

Partial differential equation (PDE) A differential equation containing multivariate functions (i.e. containing two or more independent variables) and their partial derivatives, usually of time and one or more spatial dimensions.

Performance objective An engineering analogy: A system property or target phenotype that the developmental process is intended to satisfy.

Positional information An indication of a cell's absolute location with respect to the embryo or developing organ, decoded from the local concentration of morphogenetic signal(s).

Reaction–diffusion (RD) PDE models of molecular signalling that track the spatiotemporal evolution of signal

concentrations as they react biochemically with other components of a signalling network. Transport is treated as diffusion based on assumption, approximation (as in effective diffusion) or its suggestion as the actual mechanism of transport.

Reaction-transport The generalisation of reaction–diffusion, where signalling molecule translocation may be accomplished through any mechanism.

Scale-invariance The consistent relative size of some feature with respect to the overall system size across multiple system sizes.

Source–sink model Where a morphogen is secreted from a source point or region, diffuses across a domain and is depleted in a sink point or region.

Synthesis–diffusion–degradation model Where a morphogen is secreted from a source point or region and then diffuses and reacts (is depleted) across a domain.

Top-down approach An approach to network and mechanism hypothesis building with a primary priority on exploring theoretical design principles that achieve performance objectives and an ancillary priority on their veracity in the system.

References

- Ben-Zvi D and Barkai N (2010) Scaling of morphogen gradients by an expansion-repression integral feedback control. *Proceedings of the National Academy of Sciences* **107** (15): 6924–6929. DOI: 10.1073/pnas.0912734107.
- Bollenbach T, Kruse K, Pantazis P, González-Gaitán M and Jülicher F (2005) Robust formation of morphogen gradients. *Physical Review Letters* **94** (1): 18103. DOI: 10.1103/PhysRevLett.94.018103.
- Box GEP (1979) Robustness in the strategy of scientific model building. In: *Robustness in Statistics*, pp. 201–236. New York: Academic Press.
- Carisey A, Stroud M, Tsang R and Ballestrin C (2011) Fluorescence recovery after photobleaching. In: Wells CM and Parsons M (eds) *Cell Migration: Developmental Methods and Protocols*, pp. 387–402. Totowa, NJ: Humana Press. DOI: 10.1007/978-1-61779-207-6_26.
- Crick F (1970) Diffusion in embryogenesis. *Nature* **225** (5231): 420–422. DOI: 10.1038/225420a0.
- Crowder R (1997) Mass transfer in hollow-fiber modules with non-uniform hollow fibers. *Journal of Membrane Science* **134** (2): 235–244. DOI: 10.1016/S0376-7388(97)00112-9.
- Driever W and Nüsslein-Volhard C (1988) The bicoid protein determines position in the *Drosophila* embryo in a concentration-dependent manner. *Cell* **54** (1): 95–104. DOI: 10.1016/0092-8674(88)90183-3.
- Erban R and Othmer HG (2005) From signal transduction to spatial pattern formation in *E. coli*: a paradigm for multiscale modeling in biology. *Multiscale Modeling & Simulation* **3** (2): 362–394. DOI: 10.1137/040603565.
- Frohnhöfer HG and Nüsslein-Volhard C (1986) Organization of anterior pattern in the *Drosophila* embryo by the maternal gene bicoid. *Nature* **324** (6093): 120–125. DOI: 10.1038/324120a0.

- Gierer A and Meinhardt H (1972) A theory of biological pattern formation. *Kybernetik* **12** (1): 30–39. DOI: 10.1007/BF00289234.
- Gonzalez-Gaitan M and Jülicher F (2014) The role of endocytosis during morphogenetic signaling. *Cold Spring Harbor Perspectives in Biology* **6** (7). DOI: 10.1101/cshperspect.a016881.
- Green JBA and Sharpe J (2015) Positional information and reaction-diffusion: two big ideas in developmental biology combine. *Development* **142** (7): 1203–1211. DOI: 10.1242/dev.114991.
- Gregor T, Bialek W, de Ruyter van Steveninck RR, Tank DW and Wieschaus EF (2005) Diffusion and scaling during early embryonic pattern formation. *Proceedings of the National Academy of Sciences* **102** (51): 18403–18407. DOI: 10.1073/pnas.0509483102.
- Gregor T, Wieschaus EF, McGregor AP, Bialek W and Tank DW (2007) Stability and nuclear dynamics of the bicoid morphogen gradient. *Cell* **130** (1): 141–152. DOI: 10.1016/j.cell.2007.05.026.
- Grimm O, Coppey M and Wieschaus E (2010) Modelling the bicoid gradient. *Development* **137** (14): 2253–2264. DOI: 10.1242/dev.032409.
- Hucka M, Finney A, Sauro HM, *et al.* (2003) The systems biology markup language (SBML): a medium for representation and exchange of biochemical network models. *Bioinformatics* **19** (4): 524–531. DOI: 10.1093/bioinformatics/btg015.
- Inomata H, Shibata T, Haraguchi T and Sasai Y (2013) Scaling of dorsal-ventral patterning by embryo size-dependent degradation of Spemann's organizer signals. *Cell* **153** (6): 1296–1311. DOI: 10.1016/j.cell.2013.05.004.
- Jaeger J, Surkova S, Blagov M, *et al.* (2004) Dynamic control of positional information in the early *Drosophila* embryo. *Nature* **430** (6997): 368–371. DOI: 10.1038/nature02678.
- Karim MS (2017) ProQuest Dissertations Publishing, Purdue University.
- Kicheva A, Pantazis P, Bollenbach T, *et al.* (2007) Kinetics of morphogen gradient formation. *Science* **315** (5811): 521–525. DOI: 10.1126/science.1135774.
- Le Novère N (2006) BioModels Database: a free, centralized database of curated, published, quantitative kinetic models of biochemical and cellular systems. *Nucleic Acids Research* **34** (90001): D689–D691. DOI: 10.1093/nar/gkj092.
- Lin L and Othmer HG (2017) Improving Parameter Inference from FRAP Data: an Analysis Motivated by Pattern Formation in the *Drosophila* Wing Disc. *Bulletin of Mathematical Biology* **79**: 448–497.
- Little SC, Tkačik G, Kneeland TB, Wieschaus EF and Gregor T (2011) The formation of the bicoid morphogen gradient requires protein movement from anteriorly localized mRNA. *PLoS Biology* **9** (3): e1000596. DOI: 10.1371/journal.pbio.1000596.
- Lobo D, Solano M, Bubenik GA and Levin M (2014) A linear-encoding model explains the variability of the target morphology in regeneration. *Journal of the Royal Society Interface* **11** (92): 20130918. DOI: 10.1098/rsif.2013.0918.
- Marcon L, Diego X, Sharpe J and Müller P (2016) High-throughput mathematical analysis identifies Turing networks for patterning with equally diffusing signals. *eLife* **5**: e14022. DOI: 10.7554/eLife.14022.
- Mdluli T (2017) *From Fish to Flies: Model-Based Design of Experiments and Multi-Objective Optimization for Understanding Complex Biological Systems*. West Lafayette, IN: Purdue University.
- Müller P, Rogers KW, Jordan BM, *et al.* (2012) Differential diffusivity of Nodal and Lefty underlies a reaction-diffusion patterning system. *Science* **336** (6082): 721–724. DOI: 10.1126/science.1221920.
- Newman S and Frisch H (1979) Dynamics of skeletal pattern formation in developing chick limb. *Science* **205** (4407): 662–668. DOI: 10.1126/science.462174.
- Othmer HG (1986) On the Newman-Frisch model of limb chondrogenesis. *Journal of Theoretical Biology* **121** (4): 505–508. DOI: 10.1016/S0022-5193(86)80105-9.
- Othmer HG, Dunbar SR and Alt W (1988) Models of dispersal in biological systems. *Journal of Mathematical Biology* **26** (3): 263–298. DOI: 10.1007/BF00277392.
- Othmer HG and Pate E (1980) Scale-invariance in reaction-diffusion models of spatial pattern formation. *Proceedings of the National Academy of Sciences of the United States of America* **77** (7): 4180–4184. Retrieved from <https://www.ncbi.nlm.nih.gov/pmc/articles/PMC349794/>.
- Perkins TJ, Jaeger J, Reintz J and Glass L (2006) Reverse engineering the gap gene network of *Drosophila melanogaster*. *PLoS Computational Biology* **2** (5): e51. DOI: 10.1371/journal.pcbi.0020051.
- Pomreinke AP, Soh GH, Rogers KW, *et al.* (2017) Dynamics of BMP signaling and distribution during zebrafish dorsal-ventral patterning. *eLife* **6** (Model 1): e25861. DOI: 10.7554/eLife.25861.
- Rasopovic J, Marcon L, Russo L and Sharpe J (2014) Digit patterning is controlled by a Bmp-Sox9-Wnt Turing network modulated by morphogen gradients. *Science* **345** (6196): 566–570. DOI: 10.1126/science.1252960.
- Rentzsch F (2006) Crossveinless 2 is an essential positive feedback regulator of Bmp signaling during zebrafish gastrulation. *Development* **133** (5): 801–811. DOI: 10.1242/dev.02250.
- Ries J and Schwille P (2012) Fluorescence correlation spectroscopy. *BioEssays* **34** (5): 361–368. DOI: 10.1002/bies.201100111.
- Saha K (2006) Signal dynamics in Sonic hedgehog tissue patterning. *Development* **133** (7): 1411. DOI: 10.1242/dev.02337.
- Sawala A, Sutcliffe C and Ashe HL (2012) Multistep molecular mechanism for Bone morphogenetic protein extracellular transport in the *Drosophila* embryo. *Proceedings of the National Academy of Sciences* **109** (28): 11222–11227. DOI: 10.1073/pnas.1202781109.
- Schier AF (2009) Nodal morphogens. *Cold Spring Harbor Perspectives in Biology* **1** (5): 1–21. DOI: 10.1101/cshperspect.a003459.
- Sick S, Reinker S, Timmer J and Schlake T (2006) WNT and DKK determine hair follicle spacing through a reaction-diffusion mechanism. *Science* **314** (5804): 1447–1450. DOI: 10.1126/science.1130088.
- Spirov A, Fahmy K, Schneider M, *et al.* (2009) Formation of the bicoid morphogen gradient: an mRNA gradient dictates the protein gradient. *Development* **136** (4): 605–614. DOI: 10.1242/dev.031195.
- St Johnston D, Driever W, Berleth T, Riehlstein S and Nüsslein-Volhard C (1989) Multiple steps in the localization of bicoid RNA to the anterior pole of the *Drosophila* oocyte. *Development (Cambridge, England)* **107** (Suppl): 13–19. Retrieved from <http://www.ncbi.nlm.nih.gov/pubmed/2483989>.
- Swat MH, Thomas GL, Belmonte JM, *et al.* (2012) Multi-scale modeling of tissues using CompuCell3D. In: *Methods in Cell Biology*, vol. 110, pp. 325–366. Elsevier Inc.. DOI: 10.1016/B978-0-12-388403-9.00013-8.

- Tanaka S (2015) Simulation frameworks for morphogenetic problems. *Computation* **3** (2): 197–221. DOI: 10.3390/computation3020197.
- Turing AM (1952) The chemical basis of morphogenesis. *Philosophical Transactions of the Royal Society, B: Biological Sciences* **237** (641): 37–72.
- Umulis DM, Serpe M, O'Connor MB and Othmer HG (2006) Robust, bistable patterning of the dorsal surface of the *Drosophila* embryo. *Proceedings of the National Academy of Sciences of the United States of America* **103** (31): 11613–11618. DOI: 10.1073/pnas.0510398103.
- Umulis D, O'Connor MB and Othmer HG (2008) Robustness of embryonic spatial patterning in *Drosophila melanogaster*. In: *Current Topics in Developmental Biology*, vol. **81**, pp. 65–111. DOI: 10.1016/S0070-2153(07)81002-7.
- Umulis DM (2009) Analysis of dynamic morphogen scale invariance. *Journal of the Royal Society Interface* **6** (41): 1179–1191. DOI: 10.1098/rsif.2009.0015.
- Umulis DM, Shimmi O, O'Connor MB and Othmer HG (2010) Organism-scale modeling of early *Drosophila* patterning via bone morphogenetic proteins. *Developmental Cell* **18** (2): 260–274. DOI: 10.1016/j.devcel.2010.01.006.
- Umulis DM and Othmer HG (2013) Mechanisms of scaling in pattern formation. *Development* **140** (24): 4830–4843. DOI: 10.1242/dev.100511.
- Umulis DM and Othmer HG (2015) The role of mathematical models in understanding pattern formation in developmental biology. *Bulletin of Mathematical Biology* **77** (5): 817–845. DOI: 10.1007/s11538-014-0019-7.
- Wang X, Harris RE, Bayston LJ and Ashe HL (2008) Type IV collagens regulate BMP signalling in *Drosophila*. *Nature* **455** (7209): 72–77. DOI: 10.1038/nature07214.
- Wang Y, Wang X, Wohland T and Sampath K (2016) Extracellular interactions and ligand degradation shape the nodal morphogen gradient. *eLife* **5**: 1–19. DOI: 10.7554/eLife.13879.
- Wolpert L (1969) Positional information and the spatial pattern of cellular Differentiation. *Journal of Theoretical Biology* **25**: 1–47.
- Yu SR, Burkhardt M, Nowak M, *et al.* (2009) Fgf8 morphogen gradient forms by a source-sink mechanism with freely diffusing molecules. *Nature* **461** (7263): 533–536. DOI: 10.1038/nature08391.
- Zinski J, Bu Y, Wang X, *et al.* (2017) Systems biology derived source-sink mechanism of BMP gradient formation. *eLife* **6**: e22199. DOI: 10.7554/eLife.22199.

Further Reading

- Hengenus JB, Gribskov M, Rundell AE and Umulis DM (2014) Making models match measurements: model optimization for morphogen patterning networks. *Seminars in Cell & Developmental Biology* **35**: 109–123. DOI: 10.1016/j.semcdb.2014.06.017.
- Muller P, Rogers KW, Yu SR, Brand M and Schier AF (2013) Morphogen transport. *Development* **140** (8): 1621–1638. DOI: 10.1242/dev.083519.
- Prinz H (2011) *Numerical Methods for the Life Scientist*. Berlin/Heidelberg: Springer. DOI: 10.1007/978-3-642-20820-1.
- Umulis DM and Othmer HG (2012) The importance of geometry in mathematical models of developing systems. *Current Opinion in Genetics and Development* **22** (6): 547–552. DOI: 10.1016/j.gde.2012.09.007.